Electronic Supporting Information

for

Copper(II) Complexes of Cyclams with *N*-(2,2,2-Trifluoroethyl)-aminoalkyl Pendant Arms as Potential Probes for ^{19}F Magnetic Resonance Imaging

Zuzana Kotková,[a] Filip Koucký,[a] Jan Kotek,[a]* Ivana Císařová,[a] David Parker[b] and Petr Hermann[a]

[a] Department of Inorganic Chemistry, Faculty of Science, Charles University, Hlavova 8, 128 42 Prague 2, Czech Republic. e-mail: modrej@natur.cuni.cz

[b] Department of Chemistry, Hong Kong Baptist University, Kowloon Tong, Hong Kong.

Contents

Syntheses of the alkylation agents

The *N*-(2-bromoethyl)-, *N*-(3-bromopropyl)- and *N*-(4-bromobutyl)-phthalimides were prepared by reaction of α,ω-dibromoalkane in excess (5 equiv.) with potassium phthalimide in DMF at room (ethyl derivative) or elevated (50 °C, propyl and butyl derivatives) temperatures. Volatiles were evaporated on vacuum rotary evaporator and the residues were taken up in a H_2O/EtOAc mixture. Products were isolated by evaporation of the organic phase and purified by crystallization from boiling EtOH. Less soluble bis(phthalimido)alkane by-products [*e.g.* 1,4-bis(phthalimido)butane, see Figure S2] were removed by filtration of the hot EtOH solution and the products – the alkylation agents – crystallized from the cooled solution on standing.

Characterization of the prepared compounds

The NMR spectra were acquired at 25 °C.

4,11-Dibenzyl-1,8-bis(2-phthalimidoethyl)-1,4,8,11-tetraazacyclotetradecane (1a)

Elem. anal.: Found (calcd. for **1a**, $C_{44}H_{50}N_6O_4$, M_r = 726.92). C 72.63 (72.70); H 6.70 (6.93); N 11.26 (11.56) %.

NMR ($CDCl_3$).

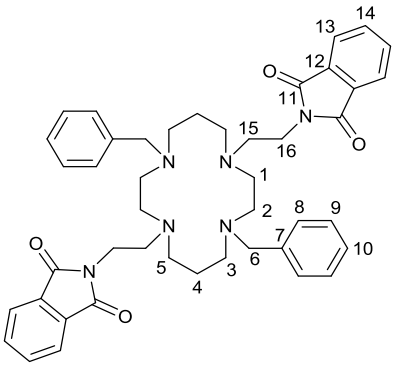

^{1}H: 1.55 (p, 4H, *H4*, $^3J_{HH}$ = 6.9); 2.39 (t, 4H, *H3*, $^3J_{HH}$ = 6.6); 2.50 (t, 4H, *H2*, $^3J_{HH}$ = 6.8); 2.53 (t, 4H, *H5*, $^3J_{HH}$ = 6.8); 2.59 (t, 4H, *H1*, $^3J_{HH}$ = 6.5); 2.61 (t, 4H, *H15*, $^3J_{HH}$ = 6.7); 3.49 (s, 4H, *H6*); 3.66 (t, 4H, *H16*, $^3J_{HH}$ = 6.7); 7.17 (t, 2H, *H10*, $^3J_{HH}$ = 7.0); 7.24 (m, 4H, *H9*); 7.26 (m, 4H, *H8*); 7.67 (m, 4H, *H14*); 7.78 (m, 4H, *H13*).

^{13}C{^{1}H}: 23.75 (s, 2C, *C4*); 36.04 (s, 2C, *C16*); 50.52 (s, 2C, *C1*); 50.98 (s, 2C, *C2*); 51.19 (s, 2C, *C3*); 51.53 (s, 2C, *C5*); 52.39 (s, 2C, *C15*); 59.57 (s, 2C, *C6*); 123.10 (s, 4C, *C13*); 126.68 (s, 2C, *C10*); 128.04 (s, 4C, *C9*); 128.98 (s, 4C, *C8*); 132.20 (s, 4C, *C12*); 133.78 (s, 4C, *C14*); 139.81 (s, 2C, *C7*); 168.30 (s, 4C, *C11*).

MS-ESI: (+) 727.7 ([**1a**+H]$^+$, calcd. 727.4).

Single crystals suitable for X-ray diffraction analysis were prepared by a slow evaporation of EtOH solution.

4,11-Dibenzyl-1,8-bis(3-phthalimidopropyl)-1,4,8,11-tetraazacyclotetradecane (1b)

Elem. anal.: Found (calcd. for **1b**, $C_{46}H_{54}N_6O_4$, M_r = 754.98). C 73.01 (73.18); H 7.02 (7.21); N 10.84 (11.13) %.

NMR ($CDCl_3$).

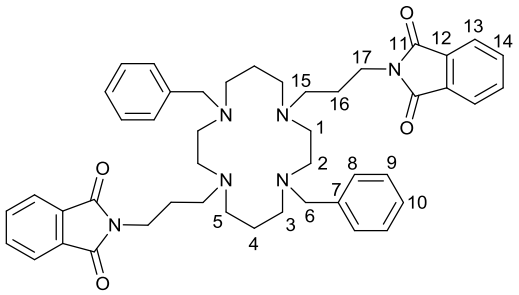

^{1}H: 1.63 (br m, 4H, *H4*); 1.73 (p, 4H, *H16*, $^3J_{HH}$ = 7.3); 2.37 (t, 4H, *H15*, $^3J_{HH}$ = 6.9); 2.46 (br m, 4H, *H5*); 2.49 (br m, 4H, *H3*); 2.51 (br s, 8H, *H1+H2*); 3.53 (s, 4H, *H6*); 3.64 (t, 4H, *H17*; $^3J_{HH}$ = 7.2); 7.20 (t, 2H, *H10*, $^3J_{HH}$ = 7.1); 7.27 (m, 4H, *H9*); 7.31 (m, 4H, *H8*); 7.69 (m, 4H, *H14*); 7.81 (m, 4H, *H13*).

^{13}C{^{1}H}: 23.46 (s, 2C, *C4*); 26.39 (s, 2C, *C16*); 36.51 (s, 2C, *C17*); 50.52 and 50.92 (s+s, 2C+2C, *C1+C2*); 51.42 and 51.46 (s+s, 2C+2C, *C3+C5*); 52.58 (s, 2C, *C15*); 59.86 (s, 2C, *C6*); 123.13 (s, 4C, *C13*); 126.73 (s, 2C, *C10*); 128.10 (s, 4C, *C9*); 128.97 (s, 4C, *C8*); 132.23 (s, 4C, *C12*); 133.80 (s, 4C, *C14*); 139.96 (s, 2C, *C7*); 168.34 (s, 4C, *C11*).

MS-ESI: (+) 755.7 ([**1b**+H]$^+$, calcd. 755.4).

Single crystals suitable for X-ray diffraction analysis were prepared by a slow evaporation of EtOH solution.

4,11-Dibenzyl-1,8-bis(4-phthalimidobutyl)-1,4,8,11-tetraazacyclotetradecane (1c)

Elem. anal.: Found (calcd. for **1c**, $C_{48}H_{58}N_6O_4$, M_r = 783.03). C 73.19 (73.63); H 7.11 (7.47); N 10.33 (10.73) %.

NMR ($CDCl_3$).

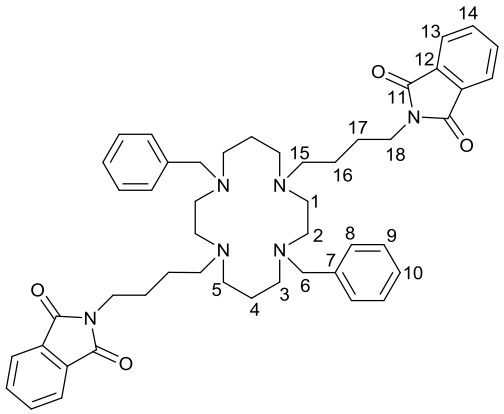

^{1}H: 1.42 (br s, 4H, *H4*); 1.62 (br s, 8H, *H16+H17*); 2.35 (br s, 4H, *H15*); 2.50 (br s, 8H, *H3+H5*); 2.58 (br s, 8H, *H1+H2*); 3.54 (s, 4H, *H6*); 3.66 (t, 4H, *H18*; $^3J_{HH}$ = 7.2); 7.21 (t, 2H, *H10*, $^3J_{HH}$ = 6.9); 7.29 (m, 4H, *H9*); 7.31 (m, 4H, *H8*); 7.73 (m, 4H, *H14*); 7.84 (m, 4H, *H13*).

^{13}C{^{1}H}: 24.74 (s, 2C, *C4*); 23.40 and 26.51 (s, 2C, *C16+C17*); 37.89 (s, 2C, *C18*); 50.42 and 50.90 (s+s, 2C+2C, *C1+C2*); 51.34 and 51.48 (s+s, 2C+2C, *C3+C5*); 54.65 (s, 2C, *C15*); 59.83 (s, 2C, *C6*); 123.14 (s, 4C, *C13*); 126.73 (s, 2C, *C10*); 128.11 (s, 4C, *C9*); 128.90 (s, 4C, *C8*); 132.16 (s, 4C, *C12*); 133.82 (s, 4C, *C14*); 139.91 (s, 2C, *C7*); 168.39 (s, 4C, *C11*).

MS-ESI: (+) 783.8 ([**1c**+H]$^+$, calcd. 783.5).

4,11-Dibenzyl-1,8-bis(2-aminoethyl)-1,4,8,11-tetraazacyclotetradecane (2a)

Elem. anal.: Found (calcd. for **2a**·6HCl·4.5H_2O, $C_{28}H_{61}N_6Cl_6O_{4.5}$, M_r = 766.53). C 43.83 (43.87); H 7.87 (8.02); N 10.80 (10.96); Cl 28.51 (27.75) %.

NMR (D_2O, hydrochloride).

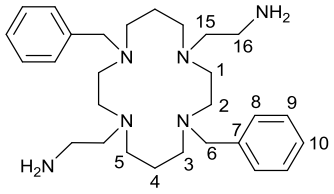

^{1}H: 2.11 (p, 4H, *H4*, $^3J_{HH}$ = 7.1); 2.84 (t, 4H, *H5*, $^3J_{HH}$ = 7.0); 2.90 (t, 4H, *H1*, $^3J_{HH}$ = 7.0); 3.08 (t, 4H, *H15*, $^3J_{HH}$ = 7.0); 3.12 (t, 4H, *H2*, $^3J_{HH}$ = 7.1); 3.41 (t, 4H, *H3*, $^3J_{HH}$ = 7.1); 3.47 (t, 4H, *H16*, $^3J_{HH}$ = 7.1); 4.47 (s, 4H, *H6*); 7.58 (br, 10H, *H8–H10*).

^{13}C{^{1}H}: 19.99 (s, 2C, *C4*); 29.59 (s, 2C, *C3*); 35.77 (s, 2C, *C2*); 45.26 (s, 2C, *C15*); 47.41 (s, 2C, *C16*); 49.39 (s, 2C, *C5*); 50.86 (s, 2C, *C1*); 58.75 (s, 2C, *C6*); 128.54 (s, 2C, *C7*); 129.51 (s, 4C, *C9*); 130.47 (s, 2C, *C10*); 131.01 (s, 4C, *C8*).

MS-ESI: (+) 467.6 ([**2a**+H]$^+$, calcd. 467.4).

4,11-Dibenzyl-1,8-bis(3-aminopropyl)-1,4,8,11-tetraazacyclotetradecane (2b)

Elem. anal.: Found (calcd. for **2b**·0.5H_2O, $C_{30}H_{51}N_6O_{0.5}$, M_r = 503.78). C 71.64 (71.53); H 9.73 (10.20); N 16.50 (16.68) %.

NMR ($CDCl_3$).

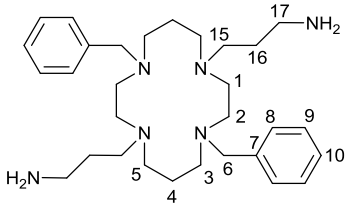

^{1}H: 1.51 (p, 4H, *H16*, $^3J_{HH}$ = 6.9); 1.70 (p, 4H, *H4*, $^3J_{HH}$ = 7.1); 2.35 (t, 4H, *H15*, $^3J_{HH}$ = 7.1); 2.50 (t, 4H, *H5*, $^3J_{HH}$ = 7.1); 2.53 (t, 4H, *H3*, $^3J_{HH}$ = 7.1); 2.58 (s, 8H, *H1+H2*); 2.66 (t, 4H, *H17*, $^3J_{HH}$ = 6.8); 3.56 (s, 4H, *H6*); 7.25 (t, 2H, *H10*, $^3J_{HH}$ = 7.1); 7.32 (m, 4H, *H9*); 7.34 (m, 4H, *H8*).

^{13}C{^{1}H}: 23.47 (s, 2C, *C4*); 31.00 (s, 2C, *C16*); 40.42 (s, 2C, *C17*); 50.54 and 50.85 (s+s, 2C+2C, *C1+C2*); 51.32 (s, 2C, *C3*); 51.44 (s, 2C, *C5*); 52.48 (s, 2C, *C15*); 59.88 (s, 2C, *C6*); 126.78 (s, 2C, *C10*); 128.10 (s, 4C, *C9*); 129.01 (s, 4C, *C8*) 139.78 (s, 2C, *C7*).

MS-ESI: (+) 495.6 ([**2b**+H]$^+$, calcd. 495.4).

A small portion of the solid material isolated after reaction of **1b** with hydrazine was re-crystallized from hot aq. EtOH, affording single crystals of phthalhydrazide salt of **2b** with composition (H_2**2b**)($C_8H_5N_2O_2$)$_2$·2H_2O suitable for X-ray diffraction.

Elem. anal.: Found (calcd. for (H_2**2b**)(phthalhydrazide-H$_{-1}$)$_2$·2H_2O, $C_{46}H_{66}N_{10}O_6$, M = 855.10). C 64.59 (64.61); H 7.66 (7.78); N 16.07 (16.38) %.

4,11-Dibenzyl-1,8-bis(4-aminobutyl)-1,4,8,11-tetraazacyclotetradecane (2c)

Elem. anal.: Found (calcd. for **2c**·6HCl·0.5H_2O, $C_{32}H_{61}N_6Cl_6O_{0.5}$, M_r = 750.58). C 51.07 (51.21); H 7.92 (8.19); N 10.97 (11.20); Cl 29.90 (28.32) %.

NMR ($CDCl_3$).

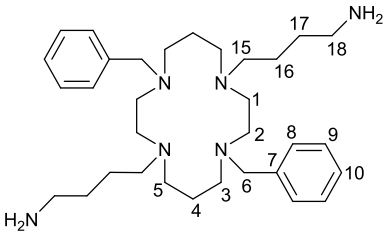

^{1}H: 1.38 (br m, 4H, *H17*); 1.39 (br m, 8H, *H16*); 1.66 (p, 4H, *H4*, $^3J_{HH}$ = 7.0); 2.33 (m, 4H, *H15*, $^3J_{HH}$ = 6.7); 2.51 (t, 4H, *H3*, $^3J_{HH}$ = 6.9); 2.53 (t, 4H, *H5*, $^3J_{HH}$ = 6.9); 2.61 (br s, 8H, *H1*+*H2*); 2.63 (t, 4H, *H18*, $^3J_{HH}$ = 6.4); 3.56 (s, 4H, *H6*); 7.24 (t, 2H, *H10*, $^3J_{HH}$ = 6.9); 7.31 (m, 4H, *H9*); 7.34 (m, 4H, *H8*).

^{13}C{^{1}H}: 23.17 (s, 2C, *C4*); 24.78 (s, 2C, *C17*); 31.71 (s, 2C, *C16*); 41.96 (s, 2C, *C18*); 50.38 (s, 2C, *C2*); 50.91 (s, 2C, *C1*); 51.27 (s, 2C, *C5*); 51.59 (s, 2C, *C3*); 55.20 (s, 2C, *C15*); 59.87 (s, 2C, *C6*); 126.75 (s, 2C, *C10*); 128.09 (s, 4C, *C9*); 128.91 (s, 4C, *C8*) 139.92 (s, 2C, *C7*).

MS-ESI: (+) 523.7 ([**2c**+H]$^+$, calcd. 523.5).

4,11-Dibenzyl-1,8-bis[*N*-trifluoroacetyl-(2-aminoethyl)]-1,4,8,11-tetraazacyclotetradecane (3a)

NMR ($CDCl_3$). ^{19}F: −74.7 (br s, *ca.* 80%); −75.2 (br s, *ca.* 20%).

MS-ESI: (+) 659.6 ([**3a**+H]$^+$, calcd. 659.4).

Single crystals of **3a** suitable for X-ray diffraction analysis were obtained by a slow evaporation of EtOH solution.

4,11-Dibenzyl-1,8-bis[*N*-trifluoroacetyl-(3-aminopropyl)]-1,4,8,11-tetraazacyclotetradecane (3b)

NMR ($CDCl_3$). ^{19}F: −75.9 (br s, *ca.* 25%); −76.3 (br s, *ca.* 75%).

MS-ESI: (+) 687.6 ([**3b**+H]$^+$, calcd. 687.4).

4,11-Dibenzyl-1,8-bis[*N*-trifluoroacetyl-(4-aminobutyl)]-1,4,8,11-tetraazacyclotetradecane (3c)

NMR ($CDCl_3$). ^{19}F: −75.8 (br s, *ca.* 51%); −75.9 (br s, *ca.* 49%).

MS-ESI: (+) 715.7 ([**3c**+H]$^+$, calcd. 715.4).

4,11-Dibenzyl-1,8-bis[*N*-2,2,2-trifluoroethyl-(2-aminoethyl)]-1,4,8,11-tetraazacyclotetradecane (4a)

NMR ($CDCl_3$). ^{19}F: −71.5 (t, $^3J_{FH}$ = 9.6).

MS-ESI: (+) 631.7 ([**4a**+H]$^+$, calcd. 631.4).

4,11-Dibenzyl-1,8-bis[*N*-2,2,2-trifluoroethyl-(3-aminopropyl)]-1,4,8,11-tetraazacyclotetradecane (4b)

NMR ($CDCl_3$). ^{19}F: −68.5 (t, $^3J_{FH}$ = 8.7).

MS-ESI: (+) 659.7 ([**4b**+H]$^+$, calcd. 659.4).

4,11-Dibenzyl-1,8-bis[*N*-2,2,2-trifluoroethyl-(4-aminobutyl)]-1,4,8,11-tetraazacyclotetradecane (4c)

NMR ($CDCl_3$). ^{19}F: −71.9 (t, $^3J_{FH}$ = 9.0).

MS-ESI: (+) 687.8 ([**4c**+H]$^+$, calcd. 687.5).

1,8-Bis[*N*-2,2,2-trifluoroethyl-(2-aminoethyl)]-1,4,8,11-tetraazacyclotetradecane (L1)

Elem. anal.: Found (calcd. for **L1**·5.5HCl·0.5H_2O, $C_{18}H_{42.5}N_6Cl_{5.5}F_6O_{0.5}$, M_r = 660.04). C 33.06 (32.76); H 6.27 (6.49); N 12.6 (12.73); Cl 29.69 (29.54) %

NMR (D_2O, hydrochloride).

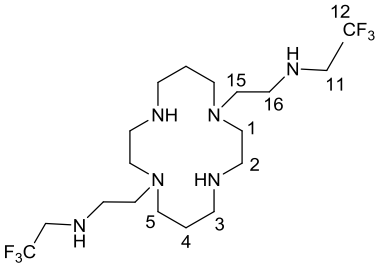

^1H: 2.03 (p, 4H, *H4*, $^3J_{HH}$ = 5.6); 2.80 (t, 4H, *H5*, $^3J_{HH}$ = 5.6); 2.94 (t, 4H, *H1*, $^3J_{HH}$ = 5.2); 3.02 (t, 4H, *H15*, $^3J_{HH}$ = 7.5); 3.22 (t, 4H, *H3*,$^3J_{HH}$ = 6.9); 3.36 (t, 4H, *H2*,$^3J_{HH}$ = 5.0); 3.44 (t, 4H, *H16*,$^3J_{HH}$ = 7.8); 4.06 (q, 4H, *H11*,$^3J_{HF}$ = 8.9).

$^{13}C\{^1H\}$: 22.84 (s, 2C, *C4*); 43.05 (s, 2C, *C16*); 43.26 (s, 2C, *C2*); 43.87 (s, 2C, *C3*); 46.24 (s, 2C, *C15*); 46.31 (s, 2C, *C1*); 47.58 (q, 2C, *C11*,$^2J_{CF}$ = 35); 49.66 (s, 2C, *C5*); 122.18 (q, 2C, *C12*,$^1J_{CF}$ = 278).

^{19}F: −68.9 (t, $^3J_{FH}$ = 8.9).

MS-ESI: (+) 451.5 ([**L1**+H]$^+$, calcd. 451.3).

Single crystals of (H_6**L1**)Cl_6·2H_2O suitable for X-ray diffraction analysis were obtained by a vapour diffusion of acetone into a solution of **L1** in aq. 10% HCl.

1,8-Bis[*N*-2,2,2-trifluoroethyl-(3-aminopropyl)]-1,4,8,11-tetraazacyclotetradecane (L2)

Elem. anal.: Found (calcd. for **L2**·6HCl·2H_2O, $C_{20}H_{50}N_6Cl_6F_6O_2$, *M* = 733.35). C 32.82 (32.76); H 6.69 (6.87); N 11.19 (11.46); Cl 30.03 (29.00) %

NMR (D_2O, hydrochloride).

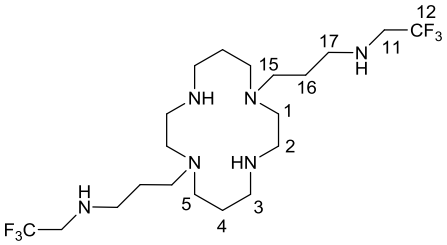

^1H: 2.10 (m, 8H, *H4*+*H16*); 3.05 (t, 4H, *H15*, $^3J_{HH}$ = 8.2); 3.11 (t, 4H, H5, $^3J_{HH}$ = 6.4); 3.24 (t, 4H, *H1*, $^3J_{HH}$ = 6.4); 3.29 (m, 4H, *H17*); 3.38 (t, 4H, *H3*, $^3J_{HH}$ = 6.9); 3.47 (t, 4H, *H2*, $^3J_{HH}$ = 6.4); 4.05 (q, 4H, *H11*, $^3J_{HF}$ = 8.8).

$^{13}C\{^1H\}$: 19.49 (s, 2C, *C16*); 20.55 (s, 2C, *C4*); 41.70 (s, 2C, *C2*); 44.79 (s, 2C, *C3*); 45.95 (s, 2C, *C17*); 47.30 (s, 2C, *C1*); 47.33 (q, 2C, *C11*, $^2J_{CF}$ = 36); 49.12 (s, 2C, *C15*); 49.67 (s, 2C, *C5*); 122.21 (q, 2C, *C12*, $^1J_{CF}$ = 278).

^{19}F: −69.0 (t, $^3J_{FH}$ = 8.8).

MS-ESI: (+) 479.5 ([**L2**+H]$^+$, calcd. 480.3).

Single crystals of (H_6**L2**)Cl_6·$2H_2O$ suitable for X-ray diffraction analysis were obtained by a vapour diffusion of acetone into a solution of **L2** in aq. 10% HCl.

1,8-Bis[*N*-2,2,2-trifluoroethyl-(4-aminobutyl)]-1,4,8,11-tetraazacyclotetradecane (L3)

Elem. anal.: Found (calcd. for **L3**·6HCl·H_2O, $C_{22}H_{52}N_6Cl_6F_6O$, *M* = 743.39). C 35.37 (35.55); H 6.68 (7.05); N 11.19 (11.31); Cl 29.00 (28.61) %

NMR (D_2O, hydrochloride).

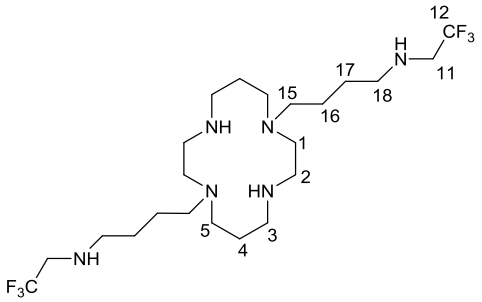

^{1}H: 1.76 (m, 4H, *H17*); 1.82 (m, 4H, *H16*); 2.11 (m, 4H, *H4*); 3.20 (t, 4H, *H18*, $^3J_{HH}$ = 7.6); 3.29 (m, 4H, *H15*, $^3J_{HH}$ = 8.0); 3.36 (t, 4H, *H3*, $^3J_{HH}$ = 8.1); 3.45 (t, 4H, *H5*, $^3J_{HH}$ = 8.3); 3.60 (m, 4H, *H2*); 3.67 (m, 4H, *H1*); 3.93 (q, 4H, *H11*, $^3J_{HF}$ = 8.8).

^{13}C{^{1}H}: 17.75 (s, 2C, *C4*); 21.25 (s, 2C, *C16*); 22.40 (s, 2C, *C17*); 36.55 (s, 2C, *C2*); 41.02 (s, 2C, *C3*); 44.46 (s, 2C, *C1*); 47.25 (q, 2C, *C11*, $^2J_{CF}$ = 35); 47.61 (s+s, 4C, *C5*+*C18*); 54.74 (s, 2C, *C15*); 122.20 (q, 2C, *C12*, $^1J_{CF}$ = 277).

^{19}F: −69.0 (t, $^3J_{HF}$ = 8.5).

MS-ESI: (+) 507.6 ([**L3**+H]$^+$, calcd. 507.4).

Determination of crystal structures by X-ray diffraction

The selected crystals of **1a**, **1b** and **3a** were mounted on a glass fibre in a random orientation and the diffraction data were collected at 150 K (Cryostream Cooler, Oxford Cryosystem) by Nonius KappaCCD diffractometer equipped with a Bruker APEX-II CCD detector using monochromatized Mo-K_α radiation (λ = 0.71073 Å). Data of other crystals were acquired at 120 K (Cryostream Cooler, Oxford Cryosystem) with Bruker D8 VENTURE Kappa Duo PHOTON100 diffractometer with an IμS micro-focus sealed tube using monochromatized Mo-K_α radiation {[Cu(H_2**L1**)](ClO_4)$_4$·$2H_2O$, [Cu(**L1**)](ClO_4)$_2$, [Cu(H_2**L2**)](ClO_4)$_4$·$2H_2O$, [Cu(**L2**)](ClO_4)$_2$, [Cu(**L3**)](ClO_4)$_2$} or with Cu-K_α radiation (λ = 1.54178 Å) {1,4-bis(phthalimido)butane, (H_2**2b**)($C_8H_5N_2O_2$)$_2$·$2H_2O$, (H_6**L1**)Cl_6·$2H_2O$, (H_6**L2**)Cl_6·$2H_2O$, {(μ-Cl)[Cu(H_2**L2**)]$_2$}(ClO_4)$_7$·$3H_2O$}.

Data were analysed using the SAINT software package (Bruker AXS Inc.). Data were corrected for absorption effects using the multi-scan method (SADABS).[1] All structures were solved by direct methods (SHELXT2014)[2] and refined using full-matrix least-squares techniques (SHELXL2017).[3]

In general, all non-hydrogen atoms were refined anisotropically. Hydrogen atoms were usually localized in difference density map. However, hydrogen atoms bound to the carbon atoms were placed in theoretical positions using U_{eq}(H) = 1.2 U_{eq}(C) to keep a number of parameters low and only hydrogen atoms bound to the heteroatoms (O, N) were usually refined. For detailed description of crystal structures of the organic compounds see ESI (Figures S2–S10 and accompanying text).

The crystal structure of [Cu(H_2**L1**)](ClO_4)$_4$·2H_2O poses centre of symmetry and, thus, one half of the formula unit form the structurally independent part. In the structure of [Cu(**L1**)](ClO_4)$_2$, the complex molecule also poses centre of symmetry but the molecule was found disordered over two positions (Figure S11). Both disordered parts share central Cu(II) ion and pivot carbon atom of the trifluoromethyl group; fluorine atoms were refined disordered over two positions. The perchlorate anion was also best refined with all oxygen atoms disordered over two positions. Despite a number of experiments to obtain crystals of kinetic isomer of complexation in the Cu^{2+}–**L2** system, only clusters/druses of very small crystals with composition {(μ-Cl)[Cu(H_2**L2**)]$_2$}(ClO_4)$_7$·3H_2O were obtained with need to disassemble them mechanically to obtain measureable single-crystals. The crystals were only poorly diffracting. For the best crystal whose data are presented in this manuscript, a total of 2569 frames were collected with the total exposure time was 19.91 hours, and only 4620 of 13563 unique reflections had intensity $I > 2\sigma(I)$, see Figure S1. In the crystal structure, whole formula unit forms the structurally independent part. One terminal trifluoromethyl group was best refined staggered in two disordered positions. Several perchlorate anions were also refined with oxygen atoms disordered over two positions and sharing the same chlorine atom. Two perchlorate anions were modelled with even chlorine atom disordered over two positions.

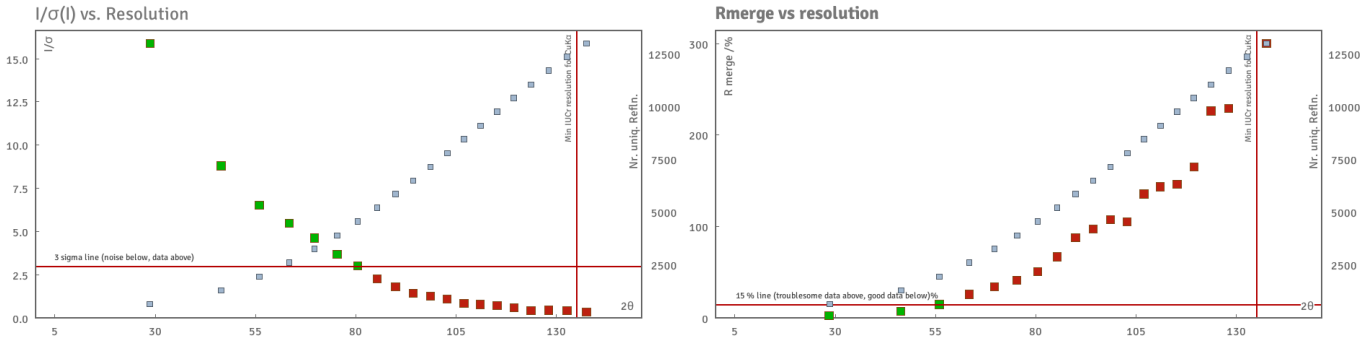

Figure S1. Graphical representation of diffraction data quality of single-crystal of {(μ-Cl)[Cu(H_2**L2**)]$_2$}(ClO_4)$_7$·3H_2O.

In the crystal structure of [Cu(H_2**L2**)](ClO_4)$_4$·2H_2O, the structurally independent part is formed by whole formula unit. One of perchlorate anions was best refined disordered over two positions sharing one of the oxygen atoms. In the crystal structure of [Cu(**L2**)](ClO_4)$_2$, two complex molecules and four perchlorate anions form the structurally independent unit. A sidearm of one of the complex molecules was found to be partly disordered over two positions, and oxygen atoms of three perchlorate anions were best refined disordered in two positions (Figure 12). Both independent complex molecules have very similar geometry (Figure S13). In the crystal structure of [Cu(**L3**)](ClO_4)$_2$, a formula unit forms the structurally independent part. Oxygen atoms of the perchlorate anions were found to be disordered over two positions and terminal trifluoromethyl groups were refined staggered in two positions.

All the data for the structures reported in this paper have been deposited with the Cambridge Crystallographic Data Centre as supplementary publication numbers CCDC-2203686–2203698. For overview of experimental crystallographic data of organic compounds see Table S1, and those of the complexes are outlined in Table S2.

Experimental crystallographic data of the reported crystal structures

Overview of experimental crystallographic data of organic compounds (ligands and intermediates) is given in Table S1 and data of the complexes are outlined in Table S2.

Table S1. Experimental data for the reported crystal structures of organic compounds.

Compound	1,4-bis(phthalimido)butane	**1a**	**1b**	$(H_2$**2b**$)(C_8H_5N_2O_2)_2{\cdot}2H_2O$	**3a**	$(H_6$**L1**$)Cl_6{\cdot}2H_2O$	$(H_6$**L2**$)Cl_6{\cdot}2H_2O$
Formula	$C_{20}H_{16}N_2O_4$	$C_{44}H_{50}N_6O_4$	$C_{46}H_{54}N_6O_4$	$C_{46}H_{66}N_{10}O_6$	$C_{32}H_{44}F_6N_6O_2$	$C_{18}H_{46}Cl_6F_6N_6O_2$	$C_{20}H_{50}Cl_6F_6N_6O_2$
M_r	348.35	726.90	754.95	855.08	658.73	705.31	733.36
Crystal system	monoclinic	triclinic	triclinic	monoclinic	monoclinic	orthorhombic	triclinic
Space group	$P2_1/c$	$P\bar{1}$	$P\bar{1}$	$P2_1/n$	$C2/c$	$Pbca$	$P\bar{1}$
a / Å	6.7363(3)	5.4701(3)	9.7722(6)	9.2066(2)	18.1534(4)	10.3077(3)	7.5009(3)
b / Å	4.7849(2)	9.6207(6)	10.0836(6)	10.8178(2)	12.3624(3)	15.2794(4)	10.4852(4)
c / Å	26.7575(12)	18.0804(9)	10.9788(7)	22.9001(5)	15.0594(4)	19.5954(5)	11.4535(4)
α / °	90	93.480(2)	74.714(3)	90	90	90	78.018(2)
β / °	110.770(2)	92.124(2)	82.564(3)	97.191(1)	103.063(1)	90	73.513(2)
γ / °	90	98.621(2)	88.502(3)	90	90	90	76.882(2)
U / Å^3	806.41(6)	937.99(9)	1034.8(1)	2262.80(8)	3292.2(1)	3086.2(1)	831.27(6)
Z	2	1	1	2	4	4	1
d (g·cm^{-3})	1.435	1.287	1.212	1.255	1.329	1.518	1.465
F_{000}	364	388	404	920	1392	1472	384
Unique refl.	2916	4294	4050	4456	3770	3040	3269
Obsd. refl.	2740	3327	3032	4028	3227	2969	3043
Parameters/restraints	119/0	244/0	253/0	304/0	212/0	230/0	209/0
$R(I>2\sigma(I))$; R'	0.0644; 0.0669	0.0409; 0.0592	0.0399; 0.0618	0.0339; 0.0373	0.0419; 0.0497	0.0295; 0.0300	0.0320; 0.0346
$wR(I>2\sigma(I))$; wR'	0.1674; 0.1686	0.0924; 0.1016	0.0894; 0.0987	0.0871; 0.0899	0.0989; 0.1048	0.0749; 0.0753	0.0794; 0.0818
CCDC ref. no.	2203686	2203687	2203689	2203697	2203694	2203698	2203688

Table S2. Experimental data for the reported crystal structures of the Cu(II) complexes.

Compound	$[Cu(H_2\mathbf{L1})](ClO_4)_4 \cdot 2H_2O$	$[Cu(\mathbf{L1})](ClO_4)_2$	$\{(\mu\text{-}Cl)[Cu(H_2\mathbf{L2})]_2\}(ClO_4)_7 \cdot 3H_2O$	$[Cu(H_2\mathbf{L2})](ClO_4)_4 \cdot 2H_2O$	$[Cu(\mathbf{L2})](ClO_4)_2$	$[Cu(\mathbf{L3})](ClO_4)_2$
Formula	$C_{18}H_{42}Cl_4CuF_6N_6O_{18}$	$C_{18}H_{36}Cl_2CuF_6N_6O_8$	$C_{40}H_{90}Cl_8Cu_2F_{12}N_{12}O_{31}$	$C_{20}H_{46}Cl_4CuF_6N_6O_{18}$	$C_{20}H_{40}Cl_2CuF_6N_6O_8$	$C_{22}H_{44}Cl_2CuF_6N_6O_8$
M_r	949.91	712.97	1873.91	977.97	741.02	769.07
Crystal system	monoclinic	monoclinic	monoclinic	monoclinic	orthorhombic	triclinic
Space group	$P2_1/n$	$P2_1/n$	$P2_1/c$	$P2_1/n$	$Pca2_1$	$P\bar{1}$
a / Å	9.2398(3)	9.0426(5)	14.8243(8)	15.0698(4)	32.570(1)	8.2745(8)
b / Å	8.7050(3)	14.8271(8)	20.508(1)	13.8170(3)	8.3885(4)	12.368(1)
c / Å	21.7616(8)	10.3300(6)	23.988(2)	17.8894(5)	21.790(1)	16.920(2)
α / °	90	90	90	90	90	108.229(3)
β / °	98.651(1)	90.231(2)	99.802(4)	99.417(1)	90	92.787(3)
γ / °	90	90	90	90	90	100.352(4)
U / Å^3	1730.4(1)	1385.0(1)	7186.1(7)	3674.7(2)	5953.4(5)	1607.7(3)
Z	2	2	4	4	8	2
d (g·cm^{-3})	1.823	1.710	1.732	1.768	1.653	1.589
F_{000}	974	734	3856	2012	3064	798
Unique refl.	3964	3188	13563	8441	13482	14497
Obsd. refl.	3888	2752	4620	7676	11985	11957
Parameters/restraints	261/0	335/50	1027/61	567/7	817/142	502/0
$R(I>2\sigma(I))$; R'	0.0277; 0.0282	0.0509; 0.0595	0.0937; 0.2520	0.0499; 0.0542	0.1033; 0.1119	0.0551; 0.0692
$wR(I>2\sigma(I))$; wR'	0.0759; 0.0763	0.1388; 0.1489	0.2022; 0.2878	0.1312; 0.1348	0.2552; 0.2614	0.1369; 0.1476
CCDC ref. no.	2203696	2203695	2203692	2203691	2203693	2203690

Description of crystal structures of organic compounds

All crystal structures of the organic compounds posse a centre of symmetry and an independent part is formed by one half of the formula unit. Some disorder was found only in the crystal structure of $(H_6\mathbf{L1})Cl_6 \cdot 2H_2O$ where the trifluoroethyl group was best refined staggered in two positions with relative occupancy 60:40%, and a water molecule of crystallization was found disordered in two close positions (71:29%).

Crystal structure of 1,4-bis(phthalimido)butane

1,4-bis(phthalimido)butane was isolated as poorly soluble by-product in preparation of *N*-(4-bromobutyl)phthalimide.

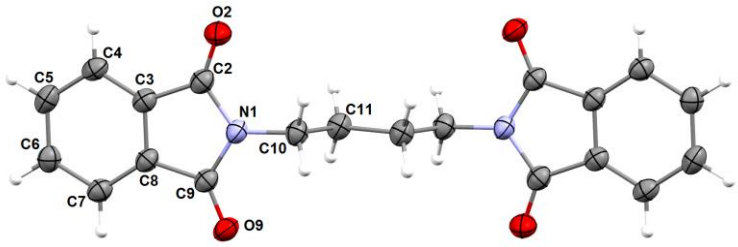

Figure S2. Molecular structure of 1,4-bis(phthalimido)butane found in its crystal structure. Only atoms belonging to the structurally independent half of the centrosymmetric molecule are labelled.

Crystal structures of 1a and 1b

Molecules of both compounds adopt centrosymmetric structure with (3,4,3,4)-B conformation of the macrocyclic backbone.[4,5] In molecule of **1a** (Figure S3), the phenyl and phthalimide moieties are roughly parallel (mutual angle 15.3°) and oriented in such a way that one carbonyl group (C18=O18) of phthalimide moiety is placed above a centroid of the phenyl group [$d(Q_{Ph}\cdots C18)$ = 3.79 Å, $d(Q_{Ph}\cdots O18)$ = 3.59 Å, Q_{Ph} is the centroid of the phenyl ring]. The second carbonyl group (C11, O11) is kept above phthalimido benzene ring of the neighbouring molecule at even slightly shorter distance [$d(Q_{phth}^{\#}\cdots C11)$ = 3.52 Å, $d(Q_{phth}^{\#}\cdots O11)$ = 3.48 Å, $Q_{phth}^{\#}$ is a centroid of the benzene ring of phthalimide group from the neighbouring molecule]. The interactions discussed above stabilize a whole crystal packing (Figure S4).

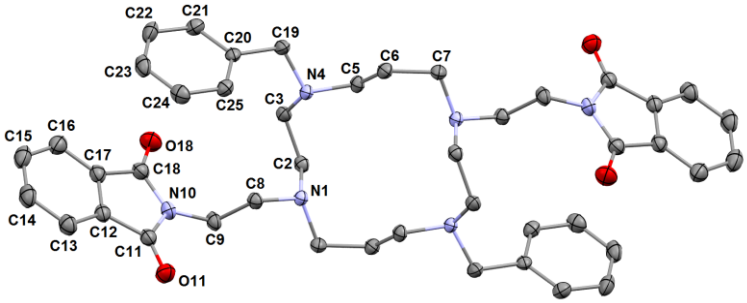

Figure S3. Molecular structure of **1a** found in its crystal structure. Hydrogen atoms are omitted for clarity. Only atoms belonging to the structurally independent half of the centrosymmetric molecule are labelled.

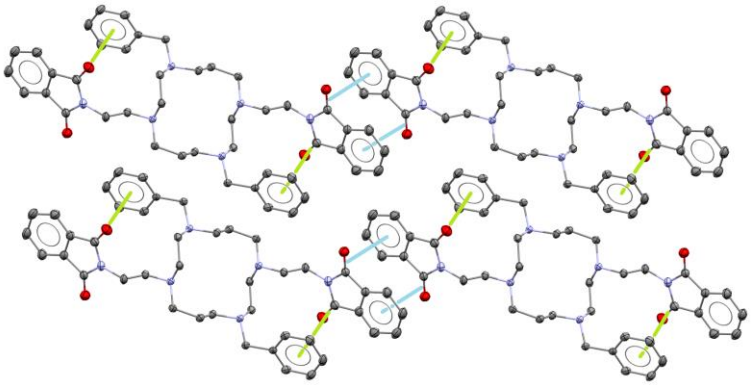

Figure S4. Carbonyl-π stacking interactions found in the crystal structure of **1a**. Hydrogen atoms are omitted for clarity. Intramolecular contacts are shown in light green, intermolecular contacts in light blue colour.

In the structure of **1b** (Figure S5), no significant intramolecular stacking interactions were found. In the crystal packing, imide nitrogen atoms caps the phenyl ring of benzyl group of the neighbouring molecule and forms a weak n-π interaction [$d(Q_{Ph}^{\#}\cdots N11)$ = 3.82 Å, $Q_{Ph}^{\#}$ is a centroid of the phenyl ring of the neighbouring molecule, Figure S6].

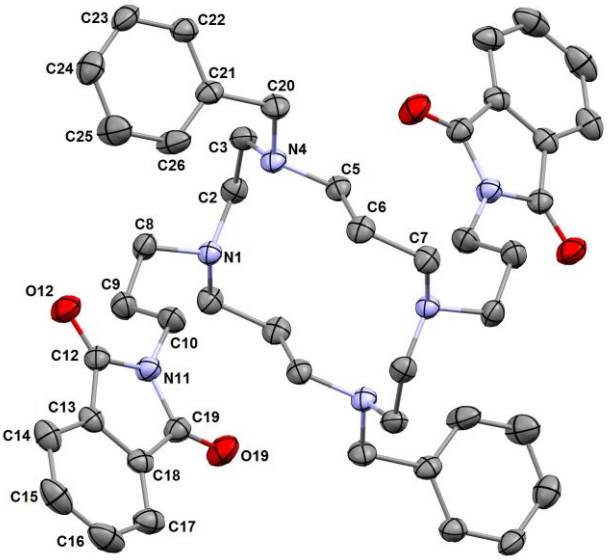

Figure S5. Molecular structure of **1b** found in its crystal structure. Hydrogen atoms are omitted for clarity. Only atoms belonging to the structurally independent half of the centrosymmetric molecule are labelled.

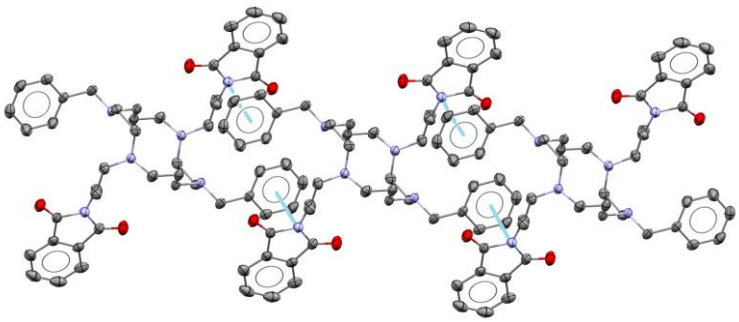

Figure S6. Lone pair-π stacking interactions found in the crystal structure of **1b** (light blue lines) Hydrogen atoms are omitted for clarity.

Crystal structure of ($H_2$2b)($C_8H_5N_2O_2$)$_2$·2H_2O

In the crystal structure of (H_2**2b**)($C_8H_5N_2O_2$)$_2$·2H_2O, the macrocyclic unit adopt centrosymmetric (3,4,3,4)-B conformation.[4,5] The primary amino groups of the 3-aminopropyl moiety are protonated, and their space orientation is stabilized by strong hydrogen bonds to the benzyl-bearing macrocycle nitrogen atom, an oxygen atom of phthalhydrazide(1−) anion and a water molecule of crystallization (Figure S7). The observed intramolecular hydrogen bond between the pendant arm and the macrocycle amino group is a common motive, whereas, usually, the proton-bearing moiety is the macrocycle amino group. Here, the rare example of proton attached to the pendant arm and the macrocycle amino group serving as an acceptor of the hydrogen bond was observed. Well-defined intermolecular hydrogen bond network form tight packing which is responsible for the low solubility to the compound.

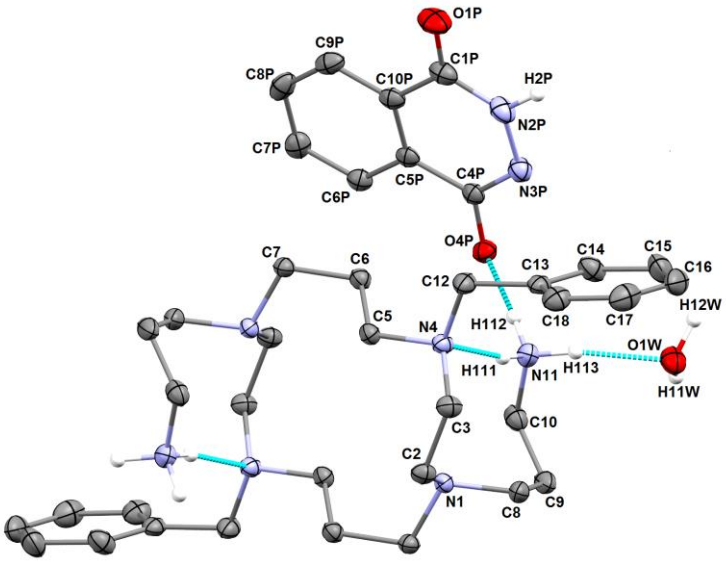

Figure S7. Selected part of the (H_2**2b**)($C_8H_5N_2O_2$)$_2$·2H_2O crystal structure. Carbon-bound hydrogen atoms are omitted for clarity. Hydrogen bonds are shown in turquoise colour. Only atoms belonging to the structurally independent half of the centrosymmetric structure are labelled.

Crystal structure of 3a

The crystal structure of **3a** revealed presence of centrosymmetric molecule in (3,4,3,4)-B conformation of the macrocyclic backbone (Figure S8).[4,5] Trifluoroacetamide group is turned to allow formation of medium-strong intramolecular hydrogen bonds between the amide nitrogen atoms and the benzyl-bearing nitrogen atoms of the macrocycle [*d*(N10···N4) = 3.27 Å]. Similarly to the previous structure, it is rare example of hydrogen bond where the macrocycle amino group serves as the hydrogen atom acceptor.

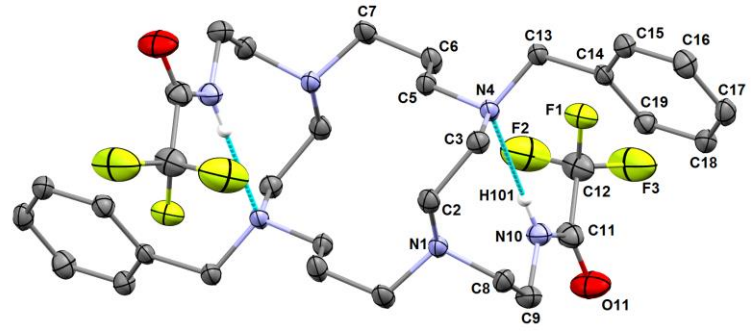

Figure S8. Molecular structure of **3a** found in its crystal structure. Carbon-bound hydrogen atoms are omitted for clarity. Intramolecular hydrogen bonds are shown in turquoise colour. Only atoms belonging to the structurally independent half of the centrosymmetric molecule are labelled.

Crystal structures of L1 and L2

The ligands **L1** and **L2** were isolated as hydrochloride salts after co-evaporation from their solution in aq. HCl, and their single-crystals were prepared from diluted aq. HCl solution on diffusion of acetone. Obtained hydrochlorides were structurally characterized (Figures S9 and S10). In the crystal structures of both compounds, all amino groups are protonated, giving analogous formulas of the solid materials, (H_6**L1**)Cl_6·$2H_2O$ and (H_6**L2**)Cl_6·$2H_2O$. In both cases, the macrocycles adopt conformation (3,4,3,4)-A with protonated amino groups located in corners of the rectangle which is the most common conformation for the fully protonated cyclam skeleton as it minimizes electrostatic repulsive forces between the protonated ring amino groups.[4,5]

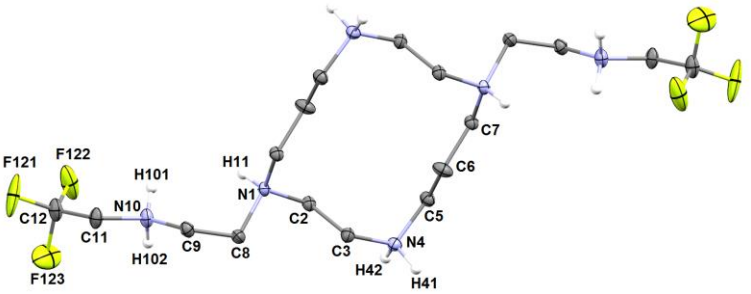

Figure S9. Molecular structure of $(H_6$**L1**$)^{6+}$ cation found in the crystal structure of (H_6**L1**)Cl_6·$2H_2O$. Carbon-bound hydrogen atoms are omitted for clarity. Only fluorine atoms of disordered trifluoromethyl group with the higher occupancy are shown, and only atoms belonging to the structurally independent half of the centrosymmetric molecule are labelled.

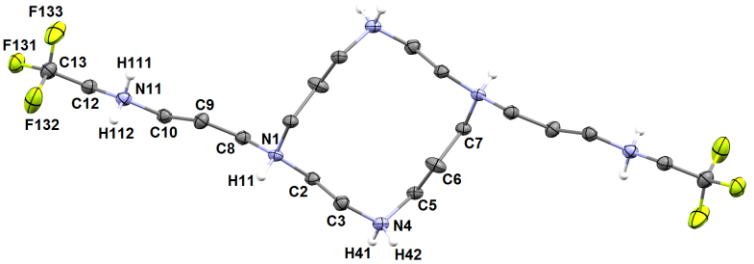

Figure S10. Molecular structure of $(H_6$**L2**$)^{6+}$ cation found in the crystal structure of (H_6**L2**)Cl_6·$2H_2O$. Carbon-bound hydrogen atoms are omitted for clarity. Only atoms belonging to the structurally independent half of the centrosymmetric molecule are labelled.

Disorders found in the crystal structures of the Cu(II) complexes

Disorder in the crystal structure of $[Cu(L1)](ClO_4)_2$

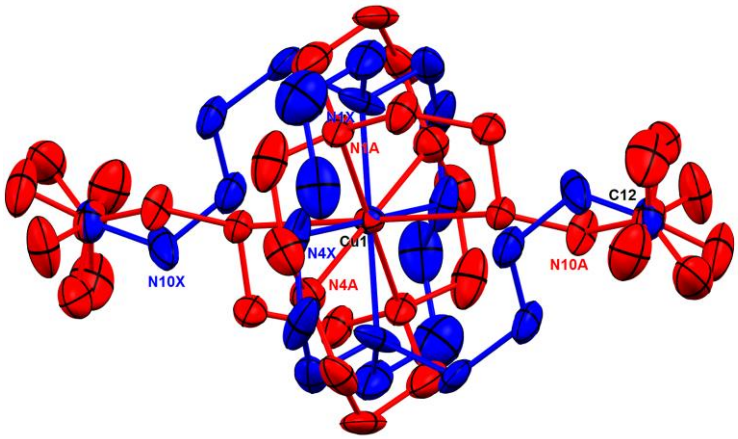

Figure S11. Molecular structure of the $[Cu(\mathbf{L1})]^{2+}$ cation found in the crystal structure of $[Cu(\mathbf{L1})](ClO_4)_2$ showing complex cation disorder. Disordered molecule possess centre of symmetry and two molecular positions share the central Cu(II) ion (Cu1) and the pivot carbon atom (C12) of the trifluoroethyl group. Hydrogen atoms are omitted for clarity, and only selected atoms are labelled.

Table S3. Selected geometric parameters found in the crystal structure of $[Cu(\mathbf{L1})](ClO_4)_2$. Donor atoms numbering rises from numbering of the cyclam ring – nitrogen atoms N1, N4, N8 and N11. The axial donors are labelled Dax1 and Dax2, respectively.

Distances (Å)		Angles (°)	
M–N1	2.080(8)/1.971(12) [c]	N1–M–N4	86.0(3)/84.1(5) [c]
M–N4	2.011(9)/2.023(11) [c]	N1–M–N8	180 [a,c]
M–N8	2.080(8)/1.971(12) [a,c]	N1–M–N11	94.0(3)/96.0(5) [a,c]
M–N11	2.011(9)/2.023(11) [a,c]	N1–M–Dax1	76.7(2)/77.0(4) [b,c]
M–Dax1	2.749(7)/2.753(11) [b,c]	N1–M–Dax2	103.3(2)/103.0(4) [a,b,c]
M–Dax2	2.749(7)/2.753(11) [a,b,c]	N4–M–N8	94.0(3)/96.0(5) [a,c]
M···F1	5.563(5)/5.558(9) [d]	N4–M–N11	180 [a,c]
M···F2	5.668(15)/5.640(29) [d]	N4–M–Dax1	94.1(3)/94.7(4) [b,c]
M···F3	6.114(7)/6.099(14) [d]	N4–M–Dax2	85.9(3)/85.3(4) [a,b,c]
M···F4	[a]	N8–M–N11	86.0(3)/84.1(5) [a,c]
M···F5	[a]	N8–M–Dax1	103.3(2)/103.0(4) [a,b,c]
M···F6	[a]	N8–M–Dax2	76.7(2)/77.0(4) [a,b,c]
		N11–M–Dax1	85.9(3)/85.3(4) [a,b,c]
		N11–M–Dax2	94.1(3)/94.7(4) [a,b,c]
		Dax1–M–Dax2	180 [a,b,c]

[a] Centrosymmetrically-related atoms (N8 = N1#, N11 = N4#, Dax2 = Dax1#, F4 = F1#, F5 = F2#, F6 = F3#, "#" means the centrosymmetric atom). [b] Axial donor is the nitrogen atom of pendant amino group (N10, Figure S11). [c] Disordered complex molecule – two positions of the ligand around common central Cu(II).

Disorder in the crystal structure of $[Cu(L2)](ClO_4)_2$

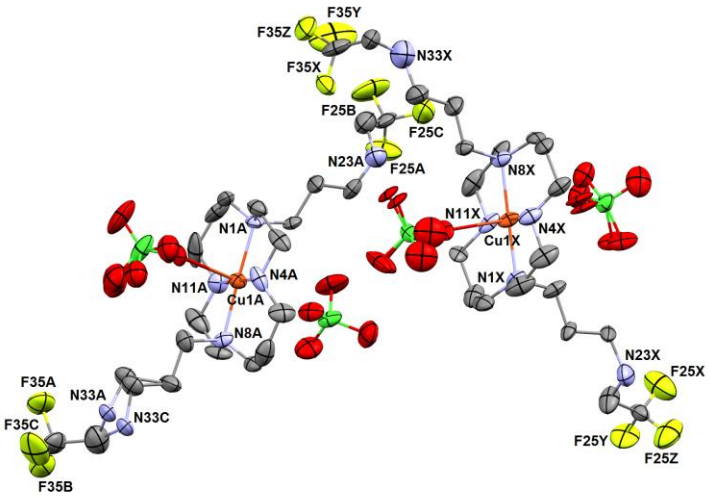

Figure S12. Crystal structure of [Cu(**L2**)]$(ClO_4)_2$ showing disorder of a pendant arm of one complex cation and that of perchlorate anions. Hydrogen atoms are omitted for clarity, and only selected atoms are labelled.

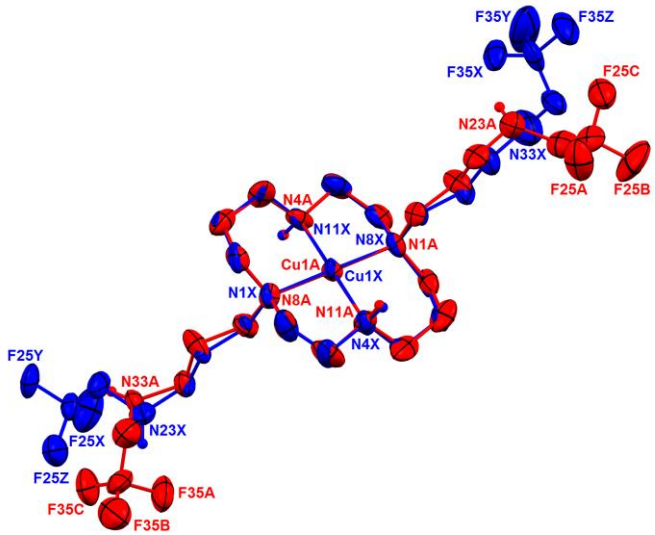

Figure S13. Overlay of two independent $[Cu(L2)]^{2+}$ complex cations found in the crystal structure of [Cu(**L2**)]$(ClO_4)_2$. Carbon-bound hydrogen atoms are omitted for clarity, and only selected atoms are labelled.

Disorders of trifluoroethyl moieties in the crystal structures of $\{(\mu\text{-Cl})[Cu(H_2L2)]_2\}(ClO_4)_7\cdot 3H_2O$ and $[Cu(L3)](ClO_4)_2$

Table S4. Selected Cu(II)···F distances found in the crystal structures of $\{(\mu\text{-Cl})[Cu(H_2\mathbf{L2})]_2\}(ClO_4)_7\cdot 3H_2O$ and [Cu(**L3**)]$(ClO_4)_2$ with disordered fluorine-containing groups. Data shows distances in the more/less occupied positions.

Parameter	$\{(\mu\text{-Cl})[Cu(H_2\mathbf{L2})]_2\}(ClO_4)_7\cdot 3H_2O$		[Cu(**L3**)]$(ClO_4)_2$
	Molecule 1	Molecule 2	
M···F1	9.475(8)	9.350(7)	10.054(3)
M···F2	9.532(9)	9.468(7)	10.344(3)
M···F3	9.903(9)	9.953(7)	11.342(3)/11.324(14)
M···F4	9.196(9)	9.19(1)/9.19(4)	10.225(8)/10.263(20)
M···F5	9.488(7)	9.49(1)/9.34(3)	10.256(6)/10.413(23)
M···F6	9.654(8)	9.69(1)/9.52(4)	11.393(5)/11.332(16)

Determination of protonation sites and protonation constants of the ligands in D_2O

Protonation sites and protonation constants of **L1** and **L2** were determined by following ^1H and ^{19}F NMR chemical shifts in dependence on "pH" in the range 2–12 ("pH" means uncorrected reading of the glass combined electrode calibrated using standard buffers in water). Samples of the ligands were dissolved in D_2O (450 μl), and "pH" was adjusted by careful addition of diluted DCl or NaOD in D_2O. In alkaline solution with "pH" > 10, the ligand **L1** slowly precipitates. Overall protonation constants defined as $\beta_n = [H_nL^{n+}]/\{[L]\cdot[H^+]^n\}$ were calculated using OPIUM program package.[6] Consecutive protonation constants are defined as $K(H_nL^{n+}) = [H_nL^{n+}]/\{[H_{n-1}L^{(n-1)+}]\cdot[H^+]\}$, and are related to the overall protonation constants by $\log K(H_nL^{n+}) = \log\beta_n - \log\beta_{n-1}$. For conversion to pK_A values, $\log K(H_nL^{n+}) = pK_A(H_nL^{n+})$.

In ^1H NMR spectra of both studied ligands, signals of the central methylene of the ring propylene group can be easily monitored as they are significantly distant from the other signals. Quartet of the methylene group of the trifluoroethyl moiety can be also assigned through entire pH range even if overlapping with other signals (it occurs in acid solutions). In addition in ^1H NMR spectra of **L2**, the central methylene group of the propylene pendant arm can be also easily identified in entire pH range used in the titration. Simultaneously, chemical shift changes of triplet present in ^{19}F NMR with pH were also analysed. The best fits of the experimental data are shown on Figure S14. The data clearly showed that the first two protonations occur in alkaline region (attributable to double protonation of the cyclam skeleton) with $\log K(H\mathbf{L1}) = 10.79(2)$ and $\log K(H_2\mathbf{L1}) = 8.74(3)$, and $\log K(H\mathbf{L2}) = 11.5(2)$ and $\log K(H_2\mathbf{L2}) = 9.12(9)$. Overall basicity of the macrocycle ring in both ligands, $\log\beta_2(\mathbf{L1}) = 19.53$ and $\log\beta_2(\mathbf{L2}) = 20.62$, is lower than that of cyclam itself ($\log\beta_2$(cyclam) = 21.48)[7] or its phosphonate derivatives,[8,9,10] but it is comparable to other cyclam derivatives as *e.g.* *N,N′,N″,N‴*-Me_4cyclam (18.38)[11] or H_4teta (20.75).[12] The lower basicity of **L1** compared to **L2** results from the shorter spacer between the macrocycle and the lectron-withdrawing substituent in the pendant arm. The third and fourth protonations obviously occur on the amino groups of the pendant arms as the processes are associated with significant chemical shift changes in ^{19}F NMR spectra and those of methylene of the trifluoroethyl moiety in ^1H NMR spectra. The "pH" dependence of the signal positions can be only successfully fitted if one common constant for both protonation steps was considered. It points that the protonations of these very distant amino groups do not mutually influence each other and both pendant arms behave independently. The fits gave protonation constants $\log K(H_3\mathbf{L1}) = \log K(H_4\mathbf{L1}) = 4.07(1)$ and $\log K(H_3\mathbf{L2}) = \log K(H_4\mathbf{L2}) = 4.82(1)$, respectively. Also in this case, length of the spacer (ethylene *vs.* propylene) between cyclam ring and the pendant amino group is reflected, leading to the lower basicity to **L1**.

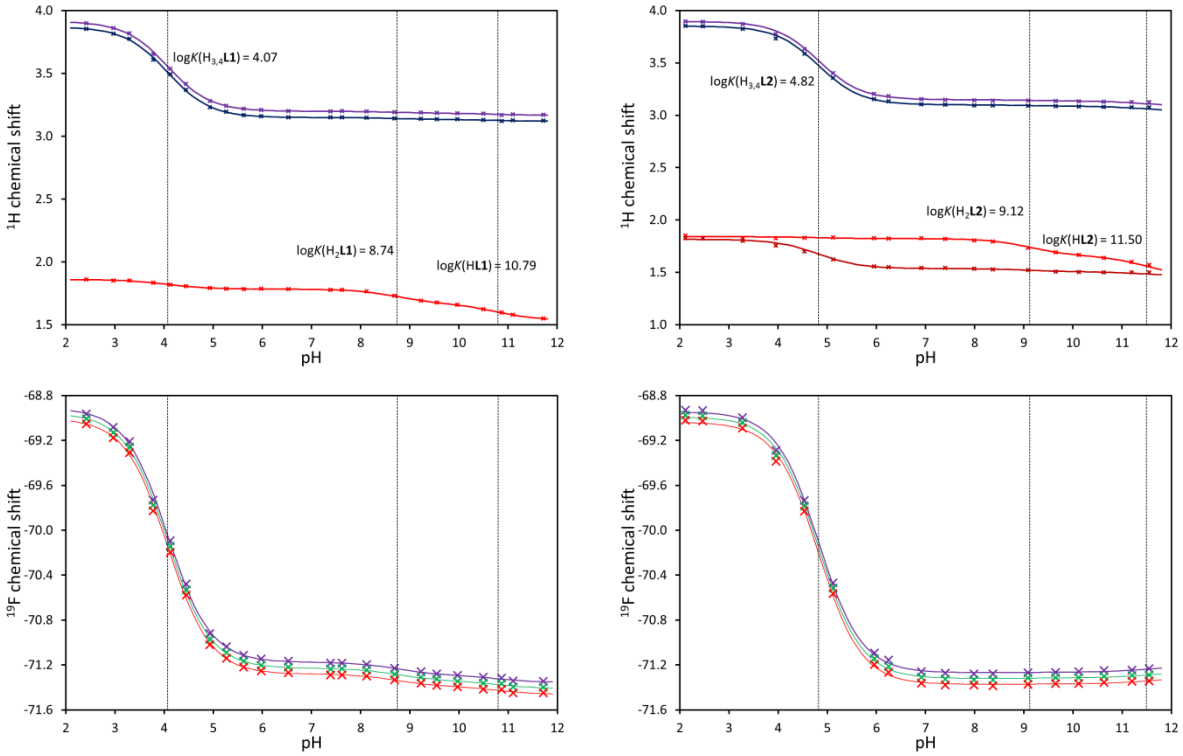

Figure S14. The pH dependence of selected signals found in ^{1}H and ^{19}F NMR spectra of **L1** (left) and **L2** (right) in D_2O. Vertical dashed lines show values of logK_a(H$_n$**L**). Colour codes: ^{1}H: blue and violet are two central lines of the quartet of CH_2CF_3 group ($^3J_{HF}$-coupling), red lines are central CH_2 group of the cyclam propylene unit, brown line is central CH_2 group of the pendant propylene unit. ^{19}F: three colours represent individual lines of triplet of the CH_2CF_3 group ($^3J_{HF}$-coupling). Crosses represent measured data, lines represent the best fits. The "pH" means direct reading of combined glass electrode (calibrated using standard buffers) immersed in D_2O solution of the samples.

Changes of visible spectra of Cu(II)–L1, Cu(II)–L2 and Cu(II)–L3 systems with time

Upon mixing of all three ligands **L1**–**L3** with a Cu(II) salt in acid aq. solution, deep blue colour was gradually developed. Upon standing the solutions at pH 3.0, colour gradually obtains reddish-violet tinge. It can be demonstrated by change in absorption spectra of the Cu(II)–**L1** system shown in Figure S15 where absorption band maximum gradually shifted from initial 565 to 550 nm during *ca.* three weeks and, then, the spectrum remains unchanged indicating that resulting violet-blue solution is fully equilibrated. The band maximum shift was also accompanied with some band narrowing. When pH of the equilibrated mixture (after 30 d) was raised to 10, the maximum of absorption band was shifted to higher energies (540 nm) and the band was slightly broadened in the long-wavelength part of the spectrum (Figure S15). This spectral change was fast (in the timescale of pH re-adjustment and spectra recording) and reversible – upon decreasing pH back to 3.0, the same spectrum as the original one before the pH increase was obtained. If pH the freshly mixed Cu(II)–**L1** system was increased to 7.4, the equilibrium was reached during one week. If the initial pH was 10, the colour change was completed overnight. In both these additional experiments, essentially the same absorption spectra were obtained for equilibrated solutions as in the first experiment (equilibration at pH 3 and later increase to pH 10) discussed above.

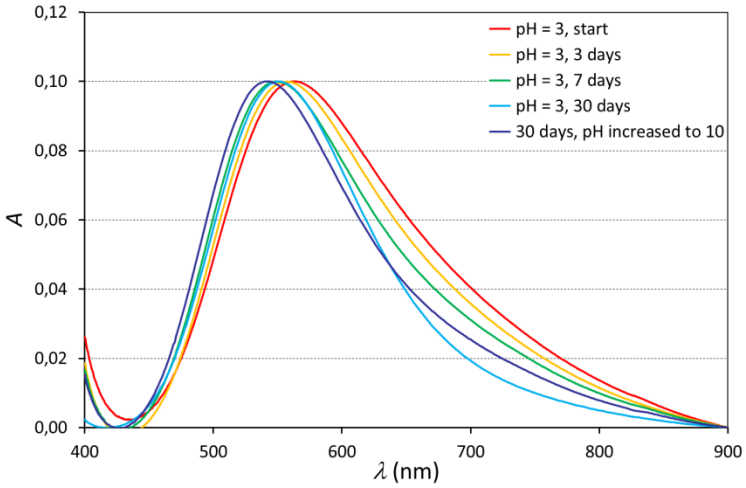

Figure S15. Time change of absorption spectra of the Cu(II)–**L1** system at pH 3, and comparison with the spectrum of the equilibrated mixture at pH 10. Spectra were scaled to same absorbance at maximum of the absorption bands to enable direct comparison of the band shapes.

The systems Cu(II)–**L2** and Cu(II)–**L3** behaved similarly. A colour change is much slower in the acid solutions compared to the neutral or alkaline ones. Spectra of fresh Cu(II)–**L2**/Cu(II)–**L3** mixtures and that of the equilibrated solutions are shown in Figure S16.

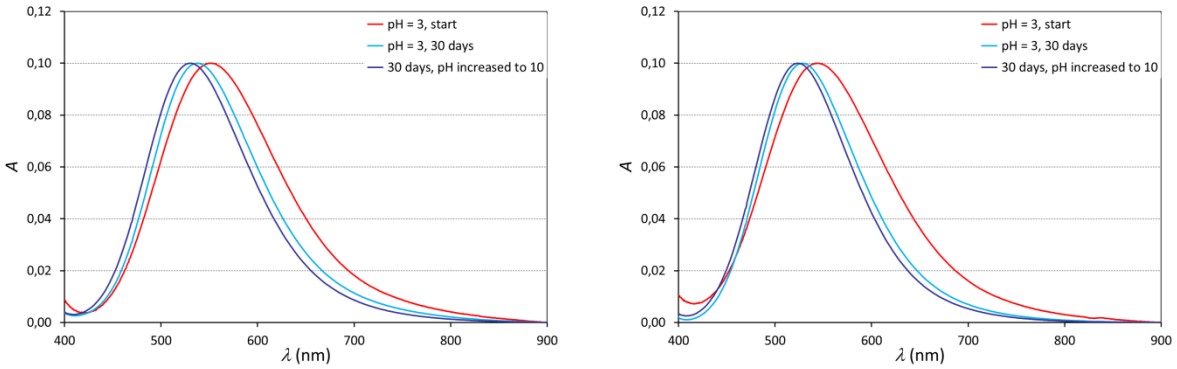

Figure S16. Change of absorption spectra of the Cu(II)–**L2** (left) and Cu(II)–**L3** (right) systems at pH 3 with time, and comparison with the spectra of the equilibrated mixture at pH 10. Spectra were scaled to same absorbance at maximum of the absorption bands to enable direct comparison of the band shapes.

Changes of ^{19}F NMR spectra of Cu(II)–L1 system with time

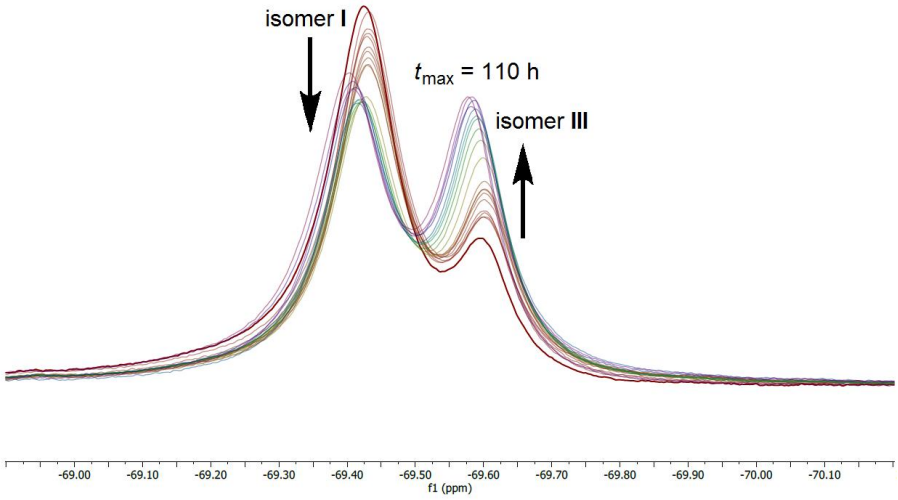

Figure S17. Changes of ^{19}F NMR spectra of the Cu(II)–**L1** system with time (pH 7.4, 50 °C, 376.1 MHz).

Changes of ^{19}F NMR spectra of Cu(II)–L1/L2/L3 complexes with pH

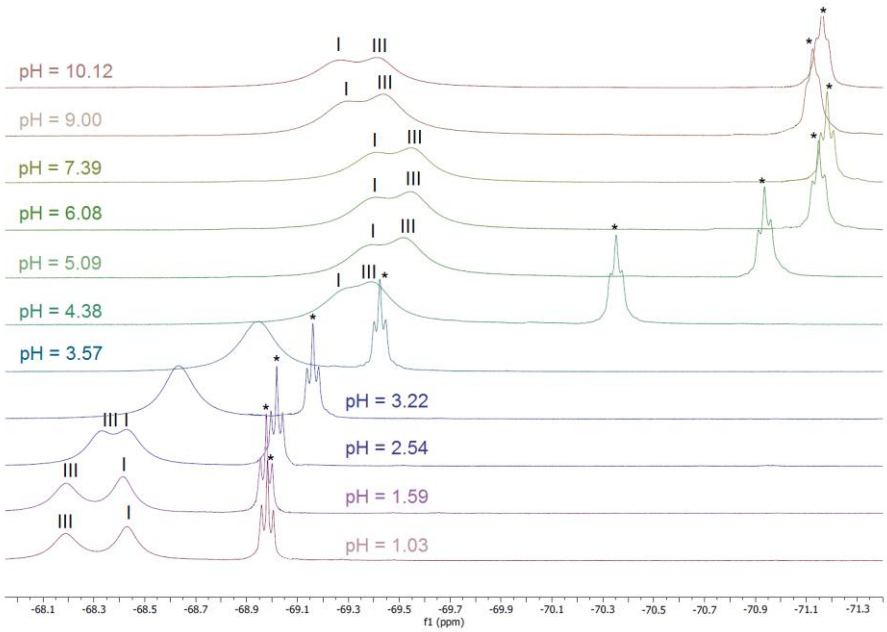

Figure S18. Dependence of ^{19}F NMR spectra of the Cu(II)–**L1** system on pH (25 °C, 376.1 MHz). Signals of individual complex species are labelled by **I** and **III**, and signal of the ligand excess is labelled by asterisk (*).

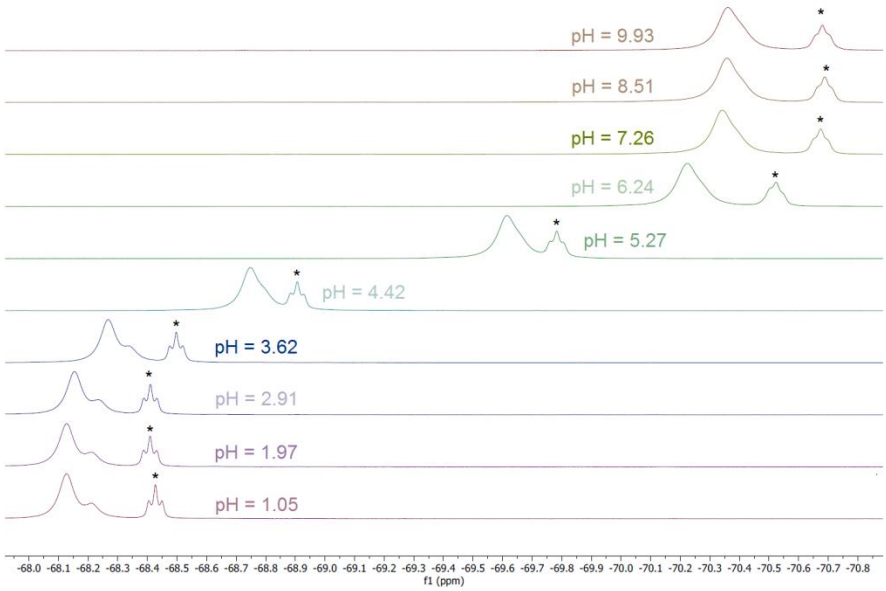

Figure S19. Dependence of ^{19}F NMR spectra of the Cu(II)–**L2** system on pH (25 °C, 376.1 MHz). Signal of the ligand excess is labelled by asterisk (*).

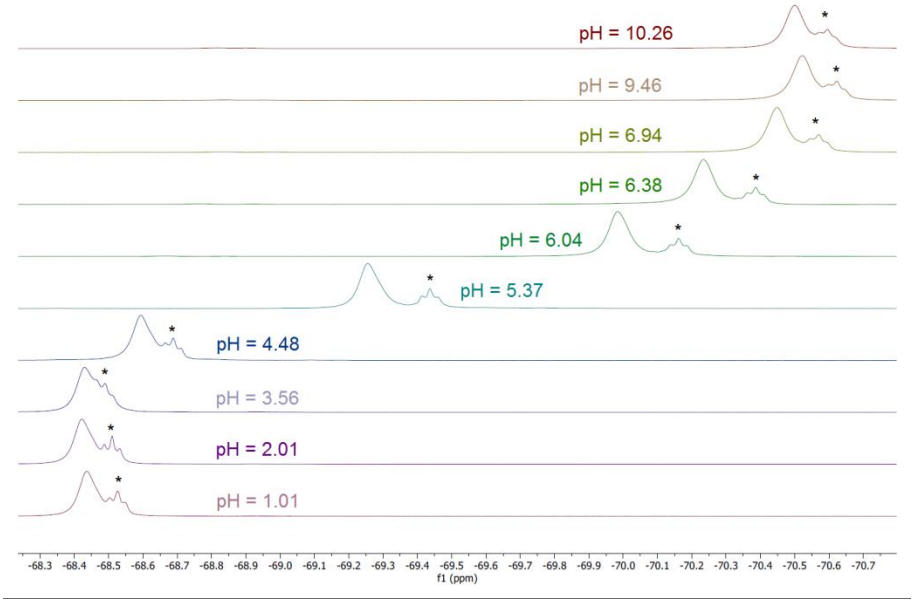

Figure S20. Dependence of ^{19}F NMR spectra of the Cu(II)–**L3** system on pH (25 °C, 376.1 MHz). Signal of the ligand excess is labelled by asterisk (*).

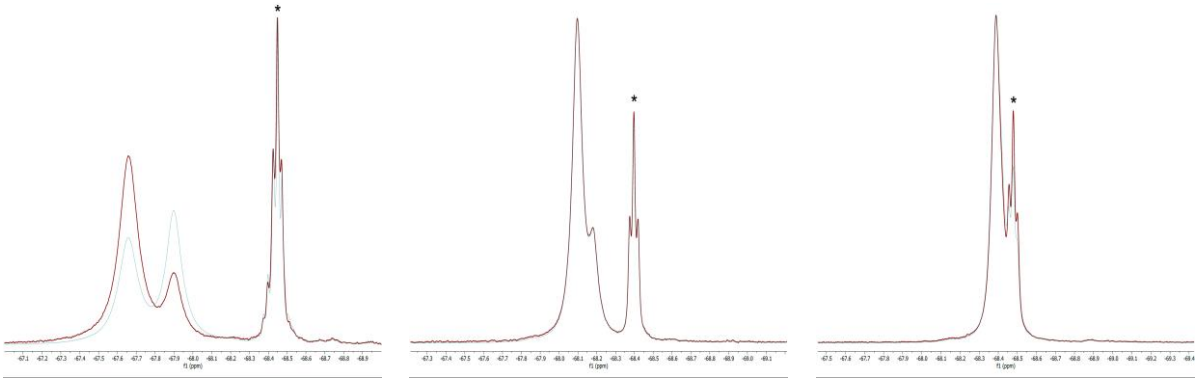

Cu(II)–**L1** Cu(II)–**L2** Cu(II)–**L3**

Figure S21. Comparison of ^{19}F NMR spectra of the Cu(II)–**L1**, Cu(II)–**L2** and Cu(II)–**L3** systems at pH 1.0. Blue line: mixtures equilibrated at neutral pH just after adjustment to pH 1.0. Red line: the same sample after two weeks at pH 1.0. The ligand excess is labelled by asterix.

Determination of dissociation constants of the ligands and complexes in H_2O

Dependence of chemical shifts on pH was fitted by OPIUM program package.[6]

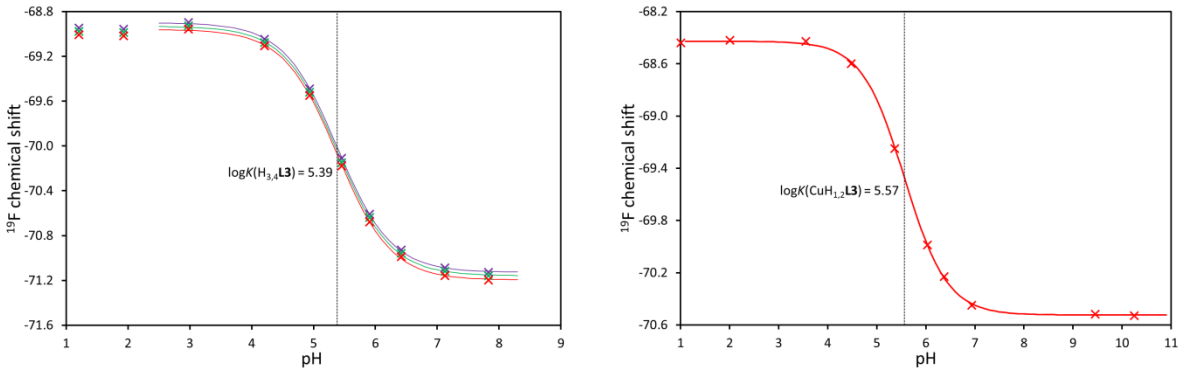

Figure S22. The pH dependence of signals in ^{19}F NMR spectra of **L3** (left) and the Cu(II)–**L3** complex (right) in H_2O. The vertical dashed lines show values of logK_a($H_{3,4}$**L3**) and logK_a($CuH_{1,2}$**L3**).

References

[1] L. Krause, R. Herbst-Irmer, G. M. Sheldrick, D. Stalke, *J. Appl. Cryst.*, 2015, **48**, 3–10.

[2] G. M. Sheldrick, *SHELXT2014/5. Program for Crystal Structure Solution from Diffraction Data*, University of Göttingen, Göttingen, 2014; G. M. Sheldrick, *Acta Crystallogr. Sect. A.*, 2008, **A64**, 112–122.

[3] C. B. Hübschle, G. M. Sheldrick and B. Dittrich, *ShelXle: a Qt graphical user interface for SHELXL*, University of Göttingen, Göttingen, 2014; C. B. Hübschle, G. M. Sheldrick and B. Dittrich, *J. Appl. Cryst.*, 2011, **44**, 1281–1284; G. M. Sheldrick, *SHELXL-2017/1. Program for Crystal Structure Refinement from Diffraction Data*, University of Göttingen, Göttingen, 2017; G. M. Sheldrick, *Acta Crystallogr. Sect. C*, 2015, **C71**, 3–8.

[4] M. Meyer, V. Dahaoui-Ginderey, C. Lecomte and R. Guilard, *Coord. Chem. Rev.*, 1998, **178−180**, 1313−1405.

[5] ComprehensiveHeterocyclicChemistry-IV_2022_Chapter14.11_591–683.

[6] M. Kývala and I. Lukeš, *Chemometrics '95*, Pardubice, Czech Republic, 1995, Abstract book p. 63; M. Kývala, P. Lubal and I. Lukeš, *IX. Spanish-Italian and Mediterranean Congress on Thermodynamics of Metal Complexes (SIMEC 98)*, Girona, Spain, 1998; full version of *OPIUM program package* is available (free of charge) from http://www.natur.cuni.cz/~kyvala/opium.html.

[7] R. D. Hancock, R. J. Motekaitis, J. Mashishi, I. Cukrowski, J. H. Reibenspies and A. E. Martell, *J. Chem. Soc. Perkin Trans. 2*, **1996**, 1925–1929.

[8] J. Kotek, P. Vojtíšek, I. Císařová, P. Hermann, P. Jurečka, J. Rohovec and I. Lukeš, *Collect. Czech. Chem. Commun.*, 2000, **65**, 1289–1316.

[9] S. Füzerová, J. Kotek, I. Císařová, P. Hermann, K. Binnemans and I. Lukeš, *Dalton Trans.*, **2005**, 2908–2915.

[10] J. Havlíčková, H. Medová, T. Vitha, J. Kotek, I. Císařová, P. Hermann, *Dalton Trans.*, **2008**, 5378–5386.

[11] A. E. Martell and R. M. Smith, *Critical Stability Constants*, Plenum Press, New York, 1974–1989, Vols. 1–6; *NIST Standard Reference Database 46* (Critically Selected Stability Constants of Metal Complexes), Version 7.0, **2003**.

[12] S. Chaves, R. Delgado, J. J. R. Frausto and Da Silva, *Talanta*, 1992, **39**, 249–254; R. Delgado, J. Costa, K. P. Guerra and L.M. P. Lima, *Pure Appl. Chem.*, 2005, **77**, 569–579.